

of the (even + $\frac{1}{2}$) angular momentum states. Figures 3(b) and 3(c) show the same contribution coming from the specific intrinsic states Φ_M^- and Φ_M^+ which generate states of, respectively, (odd + $\frac{1}{2}$) and (even + $\frac{1}{2}$) angular momentum. The density curves of the "contraster state" $\hat{\Phi}_M = U\Phi_M$ are shown in Fig. 3(d). Finally, Figs. 4(a)–4(d) show the equivalent intrinsic states of opposite deformation (prolate shape in terms of holes) which generate (here exactly) the higher energy region of this spectrum of ^{109}Ag .

It is clear that the same operator U may be considered for nonaxial deformations of odd nu-

clei.

*Also, Ministère de l'Industrie, DITEIM, Paris, France.

¹B. M. Mottelson, unpublished; cited in F. S. Stephens, R. M. Diamond, and S. G. Nilson, *Phys. Lett.* **44B**, 429 (1973).

²B. M. Mottelson, in *Nuclear Spectroscopy, Proceedings of the Enrico Fermi International School of Physics, Course XV*, edited by G. Racah (Academic, New York, 1960), p. 45.

³M. Danos and V. Gillet, *Phys. Rev.* **161**, 1034 (1967).

⁴A. Jaffrin, *Nucl. Phys.* **A196**, 577 (1972).

Electroexcitation of the Giant Resonance in ^{16}O

A. Hotta

Department of Liberal Arts, Shizuoka University, Shizuoka, Japan

and

K. Itoh and T. Saito

Laboratory of Nuclear Science, Tohoku University, Tomizawa, Sendai, Japan

(Received 15 July 1974)

Electroexcitation of ^{16}O has been measured. The strength for the $E2$ (or $E0$) resonances were extracted from the longitudinal form factors. In the region of 20–30-MeV excitation the strength exhausts approximately 20% of the sum rule for an $E2$ interpretation, while the strength in the region below 20 MeV exhausts 43% of the same sum rule. The transverse form factor is compared with calculations using both the one-particle, one-hole and the generalized Goldhaber-Teller models.

Recent experiments on the inelastic scattering of electrons, protons, and ^3He particles¹ have revealed the existence of giant quadrupole ($E2$) or giant monopole ($E0$) resonances both below and above the giant-dipole resonance in medium and heavy nuclei. The observed energies of both resonances indicate systematically $60A^{-1/3}$ or $120A^{-1/3}$ MeV dependence, respectively, and its strength exhausts more than 60% of the energy-weighted sum rule (EWSR) for an $E2$ interpretation.

In light nuclei, such evidences for a giant $E2$ resonance have not been established. A recent analysis of the reaction² $^{16}\text{O}(\gamma, n_0)^{15}\text{O}$ has shown it is necessary to assume a broad $E2$ resonance in the giant-dipole region in order to explain the angular distribution and the polarization data. Also measurements on the polarized-proton capture reaction³ $^{15}\text{N}(p, \gamma_0)^{16}\text{O}$ have shown that a broad $E2$ resonance lies above the $E1$ giant resonance and its strength exhausts approximately

30% of the $E2$ EWSR, which is a factor of 2 smaller than the prediction of the neutron data analysis. On the other hand, a study of the α -capture reaction⁴ $^{12}\text{C}(\alpha, \gamma_0)^{16}\text{O}$ has revealed a $T=0$, $E2$ strength in the region $E_x = 12$ to 28 MeV. In this Letter we present evidence for the $E2$ giant resonance in ^{16}O from a study of inelastic electron scattering.

The experiment was performed with the electron beam of the Tohoku University 300-MeV linear accelerator. Oxygen gas of 20 atm pressure, contained in a stainless-steel cylinder of 40 mm in diameter, 40 mm in height, and 0.12 mm in thickness, was used. The spectrometer and detection apparatus have been described elsewhere.⁵ The spectra of scattered electrons were taken at different angles but at the same momentum transfer in order to separate them into longitudinal and transverse parts. The overall energy resolution was 0.15%. The incident energies and scattering angles employed were 183 MeV

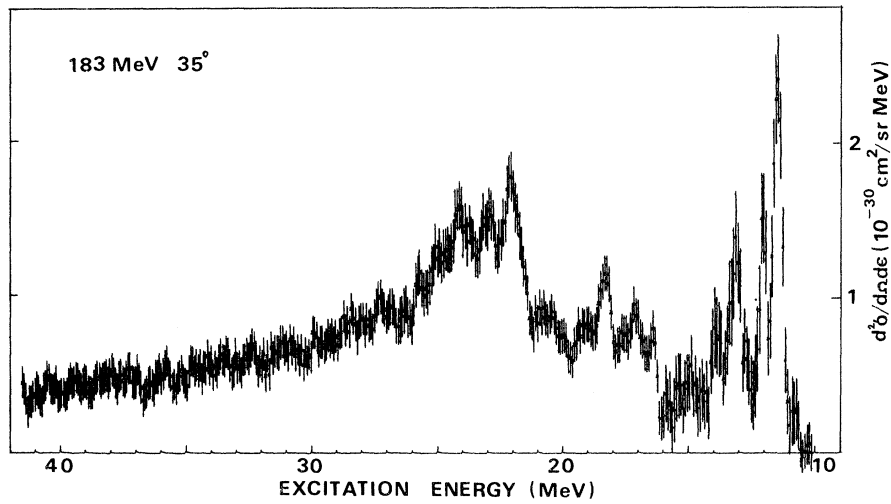


FIG. 1. Spectrum of electrons scattered from ^{16}O .

(35°), 250 MeV (40°), 250 MeV (50°), 70 MeV (120°), 97 MeV (135°), and 120 MeV (135°).

Figure 1 shows a spectrum of scattered electrons for ^{16}O at a scattering angle of 35° and an incident electron energy of 183 MeV. The domi-

nant peaks at 22.2, 23.0, and 24.3 MeV agree with the total photoabsorption γ -ray spectra of Bezić *et al.*⁶ and Agrens *et al.*⁷ The inelastic scattering cross sections were obtained by comparison with the elastic scattering cross section, whose ab-

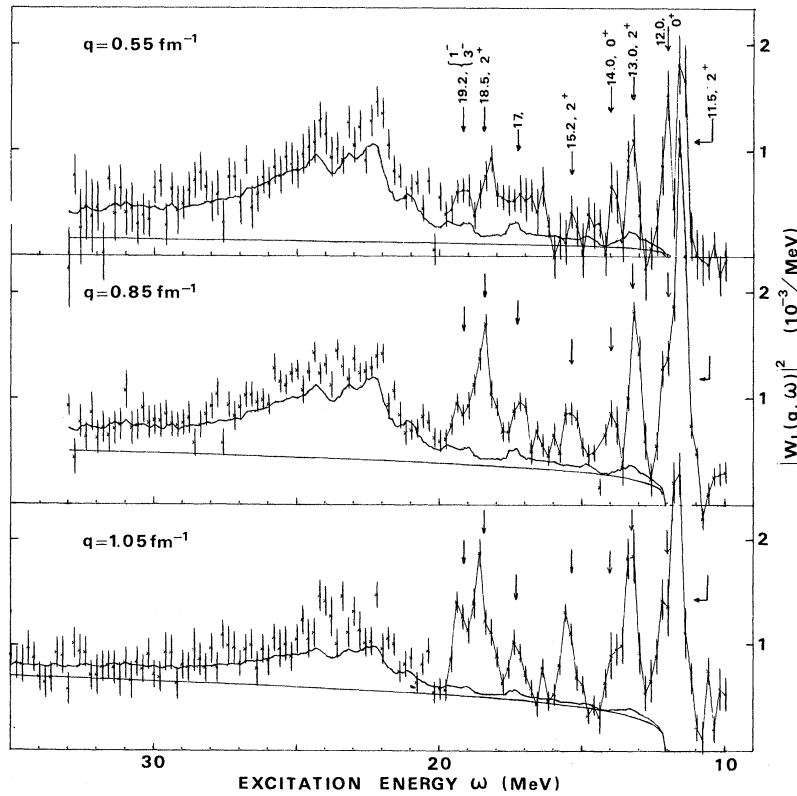


FIG. 2. The longitudinal form factors $|W_L(q, \omega)|^2$ for electroexcitation in ^{16}O from this experiment is shown as data points. The arrows show the positions of the form-factor peaks below $E_x = 20$ MeV. The middle and the lower solid curves show the total photoabsorption cross section and the continuum, respectively.

solute value was computed by phase-shift calculation using the harmonic-oscillator parameters $\alpha = 1.35$, $b = 1.81$ fm.⁸

In the Born approximation, the form factor $W(q, \omega)$ for the excitation energy ω and small energy interval $\Delta\omega$ is given by⁹

$$|W(q, \omega)|^2 = \frac{q_\mu^4}{q^4} |W_L(q, \omega)|^2 + \left(\frac{q_\mu^2}{2q^2} + \tan^2 \frac{\theta}{2} \right) |W_T(q, \omega)|^2, \quad (1)$$

where $W_L(q, \omega)$ and $W_T(q, \omega)$ are the longitudinal and transverse form factors, respectively, q_μ the four-momentum transfer of the electron, q the three-momentum transfer, ω the excitation energy, and θ the scattering angle. The usual form factor $F(q)$ is related to the form factor $W(q, \omega)$ by

$$|F(q)|^2 = \int |W(q, \omega)|^2 d\omega. \quad (2)$$

The observed spectra were normalized to a channel width of $\Delta\omega = 200$ keV, and then separated into $W_L(q, \omega)$ and $W_T(q, \omega)$ using Eq. (1).

Figure 2 shows the longitudinal form factors $W_L(q, \omega)$ as observed in this experiment for three different momentum transfers. The states of 11.5-MeV 2^+ , 12-MeV 0^+ , 14-MeV 0^+ , 15.2-MeV 2^+ , 17 MeV, 18.5-MeV 2^+ , 19-MeV 1^- , and or 3^- , and the giant-dipole resonance have been strongly excited. In this figure the *middle curve in each case* shows the total photoabsorption cross section. The q dependence of these curves was assumed to be given by the Tassie model.¹⁰ The lower curve shows the continuum which was estimated by adopting a phenomenological formula¹¹

$$y = c(E_x - E_0)^{1/n}, \quad (3)$$

where E_x is the excitation energy, $E_0 = 12.1$ MeV is the threshold energy for proton emission, n an adjustable parameter, and c is determined by fitting the sum of y and the photoabsorption cross section to the experimental spectrum at about 32 MeV.

The 18.5-MeV state has been studied by Stroetzel and Goldmann¹² who assigned to it a spin $J = 2$. The present experiment indicates that the 18.5-MeV state is strongly excited by the longitudinal component and its form factor shows a q dependence of a $E2$ -type transition. So we assign the spin and parity of this state to be $J^\pi = 2^+$.

In the giant-resonance region differences can be seen between the spectrum and the $E1$ cross section with increasing momentum transfer.

This is consistent with the existence of a higher multipole resonance besides the $E1$ giant resonance. In order to extract the strength of the

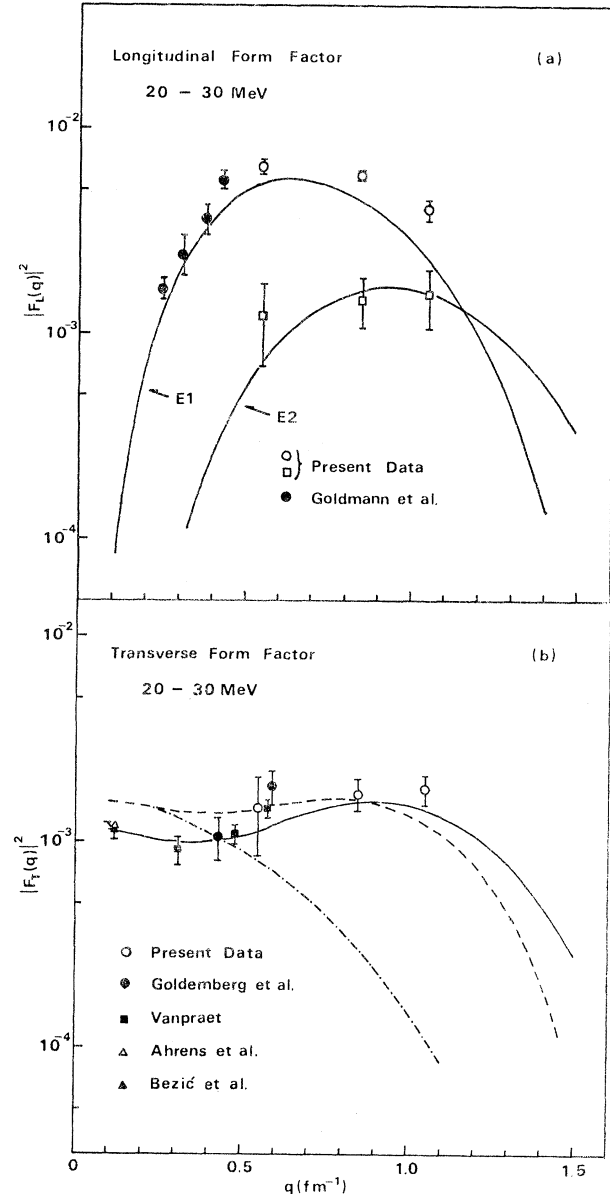


FIG. 3. (a) The longitudinal form factor for a range of 20–30 MeV as functions of q . The Darmstadt data are also plotted. The square shows the result of the subtraction of the $E1$ contribution from the experimental values. Also shown is the theoretical q dependence of the form factor for the $E1$ and $E2$ resonances. (b) The transverse form factor for the same range as for (a). The Stanford data and the photonuclear data are shown together with theoretical results calculated using the Goldhaber-Teller model (dash-dotted line), the generalized Goldhaber-Teller model (dashed line), and the particle-hole model (solid line).

TABLE I. $B(E2)$, $B(E2)$ in Weisskopf units, and energy-weighted sum-rule (EWSR) limits.

E_x (MeV)	J^π	$B(E2)$	$B(E2)/B_W(E2)$	$E_x B(E2)/EWSR$
6.92	2^+	36 ± 4^a	3.0	0.11
9.85	2^+	0.67 ± 0.27^a	0.056	0.003
11.52	2^+	25.67 ± 2.83^b	2.1	0.13
13.15	2^+	13.8^b	1.2	0.08
15.15	2^+	8.1 ± 4.1^c	0.68	0.05
16.46	2^+	2.7 ± 0.9^c	0.22	0.02
18.5	2^+	5.1 ± 0.5	0.43	0.04
			SUM	0.43
20-30	2^+	20 ± 8	1.7	0.21

^aRef. 14.^bRef. 15.^cRef. 12.

higher multipole resonance, the form factor $F(q)$ was obtained by using Eq. (2). The longitudinal form factor integrated over the region from 20 to 30 MeV is shown in Fig. 3(a) together with the low-momentum-transfer data of Goldmann and Stroetzel.¹³ Also shown in Fig. 3(a) is the $E1$ form factor calculated by using the Tassie model¹⁰ and normalizing to the data of Ahrens *et al.*⁷ The points represented by a square in Fig. 3(a) are the result of the subtraction of the $E1$ calculated contribution from the experimental values. These points are consistent with the theoretical $E2$ q dependence of the form factor given by the Tassie model.

The reduced transition probability obtained for the $E2$ resonance and a comparison with the EWSR are given in Table I together with the strengths of other 2^+ states. In this table the $E2$ strengths for the states below 16.46 MeV are taken from the data of Stroetzel,¹⁴ Kim, Singhal, and Caplan,¹⁵ and Stroetzel and Goldmann.¹²

In contrast to medium and heavy nuclei, the $E2$ strength in ^{16}O is distributed in a wide energy region. The observed strength exhausts 64% of the $E2$ EWSR, while the strength in giant-dipole-resonance region exhausts only 21% of the same sum rule. In inelastic electron scattering both isoscalar and isovector quadrupole resonances may be excited. The observed $E2$ strength above $E_x = 20$ MeV is comparable to that of the isovector giant-quadrupole resonance obtained from the (p, γ) reaction.³ Below $E_x = 20$ MeV the $E2$ strength and its distribution are in agreement with those of the isoscalar $E2$ resonances obtained from the (α, γ_0) reaction.⁴

The transverse form factor integrated over the region from 20 to 30 MeV is shown in Fig. 3(b) together with the photonuclear data^{6,7} and the

Stanford data.¹⁶ The present form factor at 0.6 fm^{-1} agrees well with the Stanford data. The transverse form factor obtained by using the Goldhaber-Teller model with the isospin mode does not agree with the data, but the form factor for the spin-isospin mode¹⁷ and the particle-hole model¹⁸ both agree with the data.

The authors would like to thank Professor Y. Torizuka and Professor Y. Kojima for their encouragements and advice.

¹See D. C. Kocher, F. E. Bertrand, E. E. Gross, R. S. Lord, and E. Newman, Phys. Rev. Lett. **31**, 1070 (1973), and references contained therein.

²W. L. Wang and C. M. Shakin, Phys. Rev. Lett. **30**, 301 (1973).

³S. S. Hanna, H. F. Glavish, R. Avida, J. R. Calarco, E. Kuhlmann, and R. LaCanna, Phys. Rev. Lett. **32**, 114 (1974).

⁴K. A. Snover, E. G. Adelberger, and D. R. Brown, Phys. Rev. Lett. **32**, 1061 (1974).

⁵M. Kimura *et al.*, Nucl. Instrum. Methods **95**, 403 (1971).

⁶N. Bezić, D. Brajnik, D. Jamnik, and G. Kernel, Nucl. Phys. **A128**, 426 (1969).

⁷J. Ahrens *et al.*, in *Proceedings of the International Conference on Nuclear Structure Studies Using Electron Scattering and Photoreactions, Sendai, Japan, 1972*, edited by K. Shoda and H. U1, CONF 720907 (Tohoku University, Sendai, Japan, 1972).

⁸J. C. Bergstrom *et al.*, Phys. Rev. Lett. **24**, 152 (1970).

⁹A. Yamaguchi, T. Terasawa, K. Nakahara, and Y. Torizuka, Phys. Rev. C **3**, 1750 (1971).

¹⁰L. J. Tassie, Aust. J. Phys. **9**, 407 (1956).

¹¹S. Fukuda and Y. Torizuka, Phys. Rev. Lett. **29**, 1109 (1972).

¹²M. Stroetzel and A. Goldmann, Z. Phys. **233**, 245 (1970).

¹³A. Goldmann and M. Stroetzel, Z. Phys. **239**, 235

(1970).

¹⁴M. Stroetzel, Z. Phys. 214, 357 (1968).¹⁵J. C. Kim, R. P. Singhal, and H. S. Caplan, Can. J. Phys. 48, 83 (1970).¹⁶J. Goldemberg and W. C. Barber, Phys. Rev. 134, B963 (1964); G. J. Vanpraet, Nucl. Phys. 74, 219 (1965).¹⁷H. Überall, Nuovo Cimento 41B, 25 (1966).¹⁸V. Gillet and N. V. Mau, Nucl. Phys. 54, 321 (1964).

New Negative Result for Gravitational Wave Detection, and Comparison with Reported Detection

James L. Levine and Richard L. Garwin

IBM Thomas J. Watson Research Center, Yorktown Heights, New York 10598

(Received 24 June 1974)

We report new negative results for detection of gravitational radiation with a 500-kg, 1637-Hz detector of demonstrated sensitivity and detection efficiency. These results are compared with numerous detections reported by Weber. We conclude that those detections did not arise from gravitational radiation. Furthermore, gravity waves (or other impulsive excitations) could not have produced data with a coincidence peak as narrow as that published in September 1973.

We report a new negative result for the detection of gravity wave pulses, at a sensitivity six times greater than that of our previous publication.¹ We believe the present results to be in substantial conflict with the detections reported by Weber²⁻⁴ although this conclusion requires estimates of Weber's detection sensitivity; his publications do not adequately present data to allow determination of the signal wave form, strength, or arrival rate (corrected for detection efficiency).

Apart from minor improvements in the transducer, the major increase in sensitivity was obtained by increasing the mass of the aluminum cylinder used as an antenna from 120 to 480 kg, the resonance frequency (1637 Hz) remaining close to that of Weber's antennae (1661 Hz). The rest of the apparatus, calibration techniques, and detection procedures are as described in Ref. 1. In particular, pulses of radiation of duration less than our 58-msec sampling interval are sought, the detection algorithm yielding the oscillation energy E_g which would be induced by a pulse in an antenna initially at rest, independently of the arrival time of the pulse and the pre-existing state of oscillation.

In Fig. 1, we show the observed impulse energies as defined above, in the form of a logarithmic histogram. The energies are determined by comparison with an electrostatic calibrator¹ and are given for convenience in units of the mean oscillation energy kT_r (T_r = room temperature), the straight line (Boltzmann distribution) being the result expected if only thermal and amplifier

noise were present. The slope of the line defines an effective temperature $T_e = 0.063T_r$ which characterizes the experiment. The histogram includes 4.1×10^7 values obtained during a 27-day period (3-30 December 1973). Only one measure-

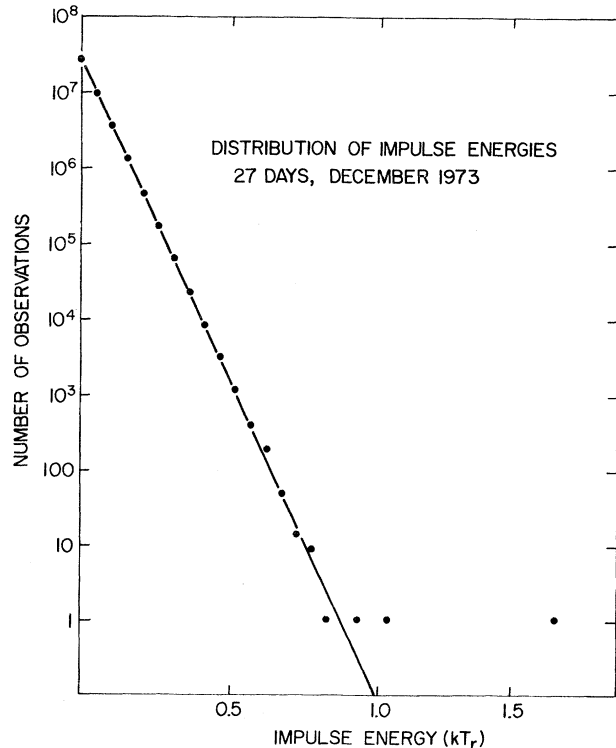


FIG. 1. Histograms of observed impulse energies. Solid curve, Boltzmann distribution with effective temperature $T_e = 18.5$ K.